



## Sol-Gel derived hybrid materials for conservation of fossils

Xiaohong Peng<sup>1,2</sup> · Yue Wang<sup>2</sup> · Xi-Fei Ma<sup>2</sup> · Haifeng Bao<sup>1</sup> · Xiao Huang<sup>1</sup> · Hongjiao Zhou<sup>3</sup> · Hongjie Luo<sup>2</sup> · Xiaolin Wang<sup>3,4,5</sup>

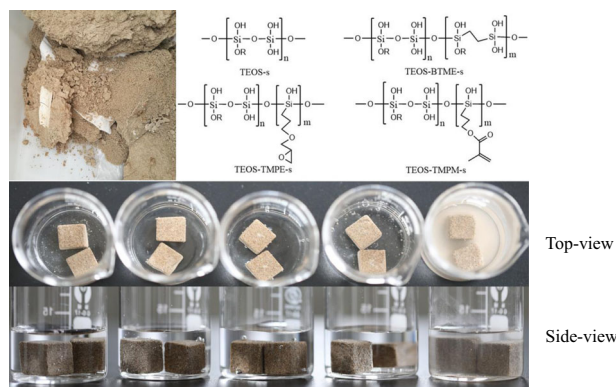
Received: 24 December 2019 / Accepted: 29 January 2020  
© Springer Science+Business Media, LLC, part of Springer Nature 2020

### Abstract

Fossils are nonrenewable natural heritages formed by Mother Nature. After being excavated or exposed, fossils can be destroyed by weathering and water erosion. However, until now, there is very limited research work on fossil conservation. In this work, we focus on the protection of pterosaur fossils found in Hami, which are very sensitive to water. Four siloxane-based polymeric sols, including from tetraethyl orthosilicate and other three hybrid siloxane monomers, are prepared by controlled hydrolysis protocol. Their chemical and physical properties and performances as fossil protection materials are examined. Experimental data show that all sols have excellent permeabilities, decent reinforcement abilities, good resistance to light and heat aging. The organic moieties in the hybrids can also significantly increase the fossil's hydrophobicity and reduce the cracking of the gels. The results indicate siloxane-based polymers can be very potential protection materials for fossils. And the hybrid polysiloxane sol containing epoxy function groups has overall the best performances.

### Graphical Abstract

Top left: severely degraded fossil due to water erosion, top right: structures of four sols Bottom: significantly improved fossil resistance to water after treated by silica sols, from left to right: treated by TEOS-TMPM-s, TEOS-TMPE-s, TEOS-BTME-s, TEOS-s and control sample.



✉ Xiao Huang  
xhuang@shu.edu.cn

✉ Xiaolin Wang  
wangxiaolin@ivpp.ac.cn

<sup>1</sup> College of Materials Science & Engineering, State Key Laboratory for New Textile Materials & Advanced Processing Technology, Wuhan Textile University, Wuhan, Hubei 430200, China

<sup>2</sup> Institute for the Conservation of Cultural Heritage, Shanghai

University, Shanghai 200444, China

<sup>3</sup> Key Laboratory of Vertebrate Evolution and Human Origins, Institute of Vertebrate Paleontology and Paleoanthropology, Chinese Academy of Sciences (CAS), Beijing 100044, China

<sup>4</sup> CAS Center for Excellence in Life and Palaeoenvironment, Beijing 100044, China

<sup>5</sup> College of Earth and Planetary Sciences, University of CAS, Beijing 100049, China

**Keywords** Sol–Gel process · Hybrid · Fossils · Conservation

## Highlights

- Four silica sols, including three hybrids sols, are synthesized via controlled sol–gel process. Their chemical and physical properties are examined.
- The as-prepared sols are applied to protect Hami fossils. It is the first systematic research on fossil protection.
- Hami fossil can be protected by these silica sols nicely and among them, hybrid sol containing epoxy function groups has overall the best performances.

## 1 Introduction

Fossils are the “evidence” of the world’s species changes and the key to human understanding of nature, playing an important role in the history of human cultural development. They have interpreted the entire process of the evolution of the earth and the development, replacement and extinction of ancient lives. The early evolutionary history of biology and the crust are documented by fossils [1]. By extracting information from fossils, we can learn more about evolution of paleoclimate [2], paleoenvironment [3] and paleogeography [4], which are of great significance in predicting the future development of the earth.

In many ways, fossils are very similar to their cousins, stone cultural relics. Both of them are basically formed by stones and contain important information which is interesting and important to human beings. They are also facing the same thermodynamic destiny. Once exposed or excavated, they will deteriorate and eventually collapse completely due to the effects from physical, chemical, biological, and anthropogenic activities [5–10]. Many studies have been carried out on the protection of stone cultural relics, to understand the weathering mechanisms, to slow down the weathering process and extend their lifetime [11–17]. And such research work is still going on. But, unfortunately very little related protection work has been done on fossils.

Factors such as wind [6], rain [18], underground water, soluble mineral salts [8, 9], environmental pollutions [7, 19], microorganism [10] and dramatic environmental changes before and after excavation are the major possible causes for deterioration of stone heritages. And among these factors, efflorescence from water is a serious threat and of particular importance. Water, not only itself can do damages to those relics, but also can further arise problems caused by soluble salts, microorganism etc. Reinforcement of the weathered relics and water-resistance treatments are often applied to against water-induced erosion.

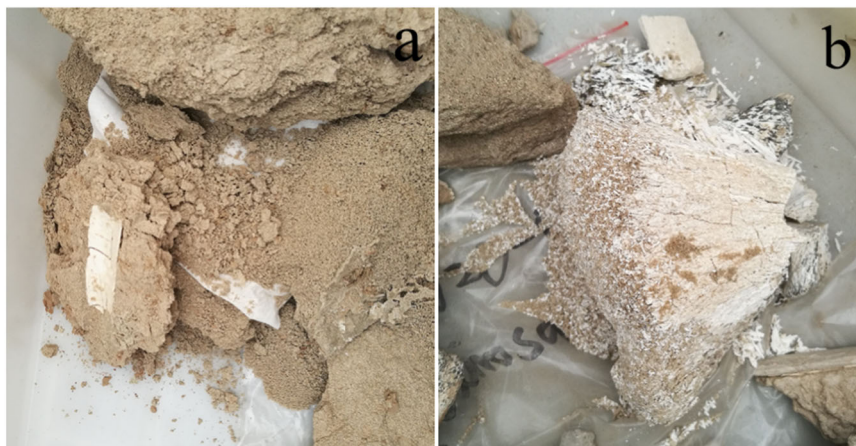
Simple siloxanes such as ethyl orthosilicate and their oligomers have been widely applied in stone conservations because they will eventually convert to silica, a major component of silicious stones [20–22]. Meanwhile, such

materials have fairly low viscosity, so that they can wet the stone surface and penetrate into the stone well to guarantee good reinforcement. For example, Grissom et al. [23] used the ethyl silicate solution to consolidate the ancient stone statue fragments, which remained intact after 11 years. Saleh et al. [24] used methyl trimethoxy silane to achieve good results in the protection of Egyptian sandstone. However, the simple siloxanes or oligomers tend to form brittle and rigid gels. Obvious weight loss and volumetric shrinkage during curing make them susceptible to crack and may accelerate the destruction of cultural heritages [25–28]. Avoiding cracking during curing is still a major research focus of siloxane-based materials in stone consolidation applications [29–32].

More recently, organosiloxane-based hybrid materials have attracted a lot of attention because of their unique molecular structures, which mainly consist of both Si–O–Si bonds and some organic functional groups [33, 34]. When applied, the Si–O bonds will combine with the stones to restore the mechanical integrity as simple siloxane molecules do, while the organic groups can provide certain type of protective function, for example hydrophobicity. Furthermore, the organic groups can reduce the amount of weight and volume loss, and provide some flexibility to the rigid silica gel network, thus to weaken cracking.

After more than 10 years of investigation and research, a large number of vertebrate fossils represented by pterosaurs (*Hamipterus tianshanensis*) were discovered in Hami, Xinjiang, including the first 3D pterosaur egg and embryo in the world [35, 36]. This is one of the most exciting discoveries of pterosaur research in 200 years. The discovery represents a unique opportunity to investigate pterosaur growth, development, reproductive behavior and ecology [37], and is a crucial advance in understanding pterosaur reproduction [38]. However, during research it was found that many of these precise fossils started to decay. Shortly after their excavation and transportation from Hami to laboratories in Beijing, severe degradation such as surface powdering, spalling and disintegration occurred (Fig. 1). Previous research shows that the deterioration of these fossils is mainly due to water erosion [39]. It was found that the fossil and matrix acquired in Hami had very

**Fig. 1** Severe weathered samples after being transported from Hami to Beijing. **a** Matrix (the white parts are fossils); **b** Pterosaur fossil



poor resistant to water. Meanwhile, wind erosion is the major cause for Hami fossil weathering in the field.

In this work, for the purpose of Hami fossil protection, several sol-gel derived hybrid materials are prepared from organosiloxane monomers. Their abilities of fossil conservation are evaluated.

## 2 Experimental

### 2.1 Materials

Tetraethyl orthosilicate (TEOS, 98%) was purchased from Macklin Co. Bis(trimethoxysilyl)ethane (BTME) was obtained by Wuda Organic Silicon New Materials Co. (3-Aminopropyl) trimethoxysilane (TMA, 97%),  $\gamma$ -(2,3-epoxypropoxy) propyltrimethoxysilane (TMPE, 97%) and 3-(Trimethoxysilyl) propyl methacrylate (TPM, 97%) were acquired from Aladdin Co. Anhydrous ethanol (>99.9%, AR) and hydrochloric acid (36–38%, AR) were purchased from Sinopharm Co. All reagents were used as received without further purification.

The pterosaur fossils and matrices were collected from Hami, Xinjiang. Before usage, the matrices were cut into 10\*10\*10 mm cubic blocks.

### 2.2 Characterizations

X-Ray Fluorescence (XRF) was recorded by a Niton XL3t spectrometer (Thermo Fisher Scientific Co.). The X-ray diffraction (XRD) analyses were performed using a PANalytical AERIS X-ray Diffractometer. Viscosities were measured by a Rotational viscometer (Smart series, ChemTron Co.) at 25 °C. Fourier-transform infrared spectra (FT-IR) were recorded on a Nicolet iS50 spectrometer over a spectrum range from 4000 to 400  $\text{cm}^{-1}$ .  $^{29}\text{Si}$  NMR spectra were collected at room temperature in  $\text{CDCl}_3$  with a Bruker AVANCE III HD 600 MHz spectrometer. Photos were

**Table 1** Composition of the organosiloxane sols in molar ratios

Monomer	TEOS	BTME	TMPE	TMPM
Sol				
TEOS-s	1	0	0	0
TEOS-BTME-s	1	1	0	0
TEOS-TMPE-s	1	0	1	0
TEOS-TMPM-s	1	0	0	1

taken by a Canon EOS 5D MARK IV camera. Thermogravimetric analyses (TGA) were recorded on an STA 449 F3 thermal analyzer (Netzsch Co.). The Leeb hardness was measured by a CXJ-30 pen type hardness tester. Water contact angles of the samples were determined using a contact angle goniometer (OCA15EC, Dataphysics). Compressive strength was measured by a Zwick BZ2.5/TS1S material testing machine. The chromatic aberration was measured by a I5 desktop spectrophotometer (X-Rite, USA).

### 2.3 Preparation of hybrid sols

Four kinds of sols synthesized from different organosiloxane monomers are listed in Table 1. Monomers were first added into anhydrous ethanol (molar ratio of monomer/anhydrous ethanol = 1/2.6) under magnetic agitation. Then, they were stirred for 10 min before 0.1 M HCl solution (60% hydrolysis degree of organosiloxane monomer) was added dropwisely. After the completion of addition, all the samples were kept under magnetic agitation at 70 °C for 10 h. All sols are prepared as the molarities of Si are the same. Figure 2 shows the proposed molecular structures of the four organosiloxane-based hybrid sols.

**Fig. 2** Proposed molecular structures of four hybrid sols (R = methyl/ethyl)

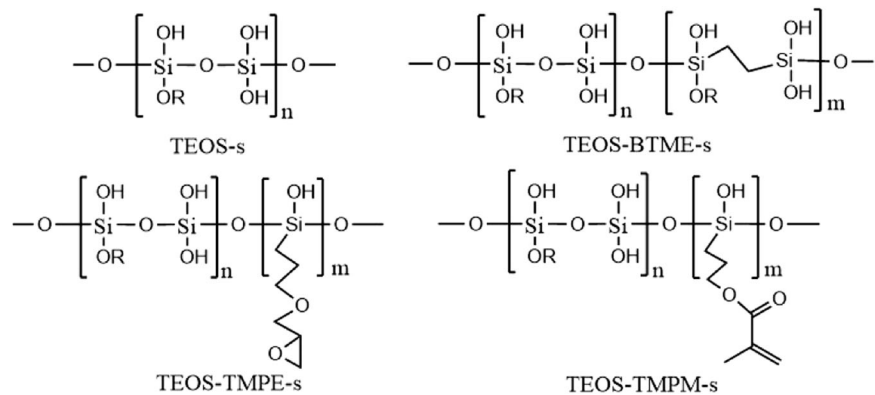


**Table 2** XRF analyses of matrix and fossil samples from Hami

Chemical composition	Weight (%)	
	Matrix	Fossil
Si	31.22	7.1
Ca	11.72	37.18
Al	4.41	1.85
Fe	3.4	0.31
K	1.17	0.16
Mg	1.1	–
Ti	0.3	0.02
Cl	0.23	0.04
P	–	14.06

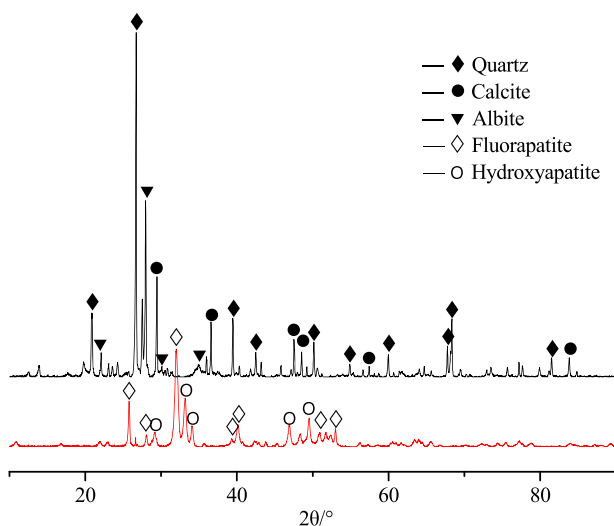


**Fig. 3** XRD patterns of the matrix (black) and fossil (red)

## 2.4 Consolidation evaluation

Immersion method is adopted since it is very convenient and practical to perform in laboratory. Since fossils are precious, matrices are used as simulated samples instead.

Two sets experiments were performed. Matrix blocks were soaked in as-prepared four consolidants for 10 min respectively. 5 wt% TMA was used as catalyst in all cases. All consolidated samples were aged at ambient conditions for 24 h to ensure that the sol–gel processes were complete. After reaction completion, the amount of final consolidant is around 3.5 wt% of the matrices.

The effect of consolidation was indicated by compressive strength, measured according to ASTM C170/C170M-09.

The aging-resistance was evaluated at two conditions, respectively: exposure under a UV lamp (365 nm) at the distance of 15 cm or in a 60 °C oven. Color alteration was followed as an indication of photo and thermal aging. The reported chromatic aberration was the average of the measured values of the three individual samples. The color difference E was calculated by Eq. (1):

$$\Delta E = \left[ (\Delta L^*)^2 + (\Delta a^*)^2 + (\Delta b^*)^2 \right]^{0.5}, \quad (1)$$

where  $L^*$ ,  $a^*$  and  $b^*$  are the measured parameters:  $L^*$  is brightness,  $a^*$  and  $b^*$  are coordinates ( $a^*$  is the red–green parameter and  $b^*$  is the blue–yellow).

## 3 Results and discussions

### 3.1 Characterization of pterosaur fossils and matrices

XRF and PXRD results of fossil and matrices are summarized in Table 2 and Fig. 3. The matrices mainly consist of quartz and calcite, while the fossils mainly consist of fluorapatite and hydroxyapatite. The XRF and PXRD data are totally consistent with each other.

### 3.2 Organosiloxane sols characterization

For consolidation purpose, it is important for sols to penetrate into the fossils. Viscosities strongly influence their

**Table 3** Viscosities of the organosiloxane sols<sup>a</sup>

	TEOS-s	TEOS-BTME-s	TEOS-TMPE-s	TEOS-TMPM-s
Viscosities (cP)	1.8	3.0	1.9	2.2

<sup>a</sup>The molarities of Si in the sols are the same

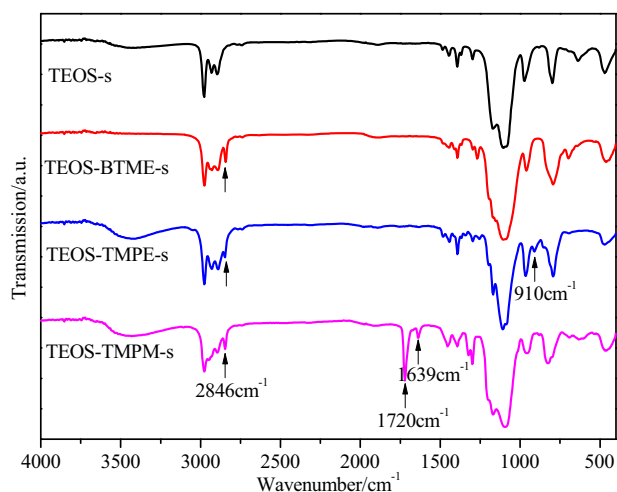


**Fig. 4** FT-IR of the organosiloxane sols: TEOS-s, TEOS-BTME-s, TEOS-TMPE-s and TEOS-TMPM-s

penetration behaviors and also are indications of their molecular weights, which are controlled by the degree of hydrolysis with respect to the moles of siloxane monomers. The as-prepared sols have fairly low viscosities which will allow them to easily enter the interior of the fossils (Table 3).

The sols are further characterized by FT-IR after removal of solvents, as shown in Fig. 4. Broad peaks around  $3500\text{ cm}^{-1}$  are due to the  $-\text{OH}$  groups after hydrolysis of the monomers. Adsorption bands around  $2800\text{--}3000\text{ cm}^{-1}$  are asymmetry stretching vibrations of C-H, among which bands at  $2846\text{ cm}^{-1}$  only observed in three hybrid sols are vibrations of C-H in the organic function groups. The characteristic adsorption peaks of the Si-O-Si around  $1000\text{--}1300\text{ cm}^{-1}$  are clearly observed in all four sols, indicating the occurrence of condensations. The characteristic peaks of acrylate (carbonyl at  $1720\text{ cm}^{-1}$  and C=C at  $1639\text{ cm}^{-1}$ ) and epoxy groups ( $910\text{ cm}^{-1}$ ) can also be observed nicely in TEOS-TMPE-s and TEOS-TMPM-s, respectively.

$^{29}\text{Si}$  NMR is a powerful tool for the investigation of the chemical bonding environments of Si atoms of organosiloxane sols, given the complex chemistry involved in the sol-gel process. According to the number of O atoms connected with Si atoms, Si can be classified into four types:  $M_n$  (monofunctional),  $D_n$  (difunctional),  $T_n$  (trifunctional) and  $Q_n$  (quaternary), in which the subscript “ $n$ ”

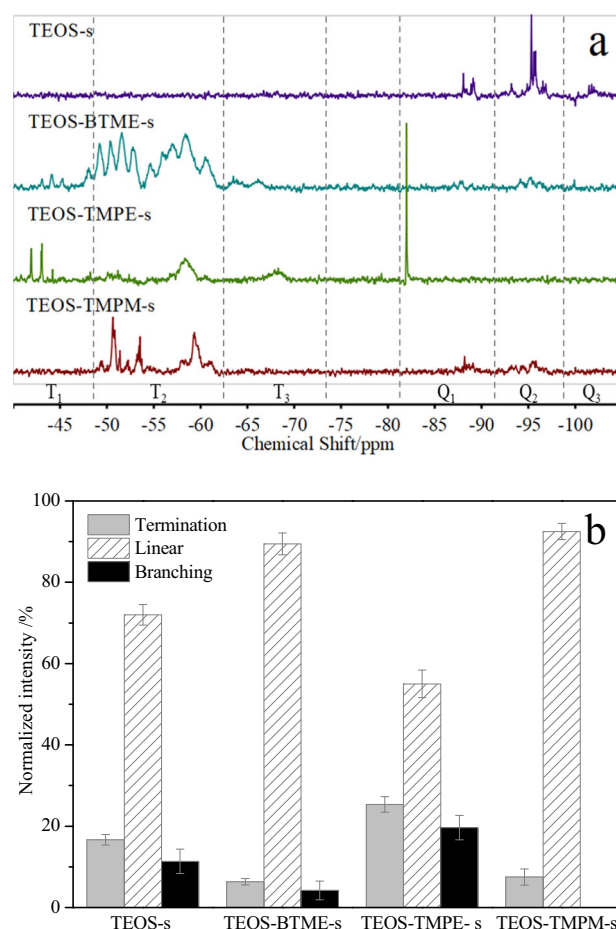
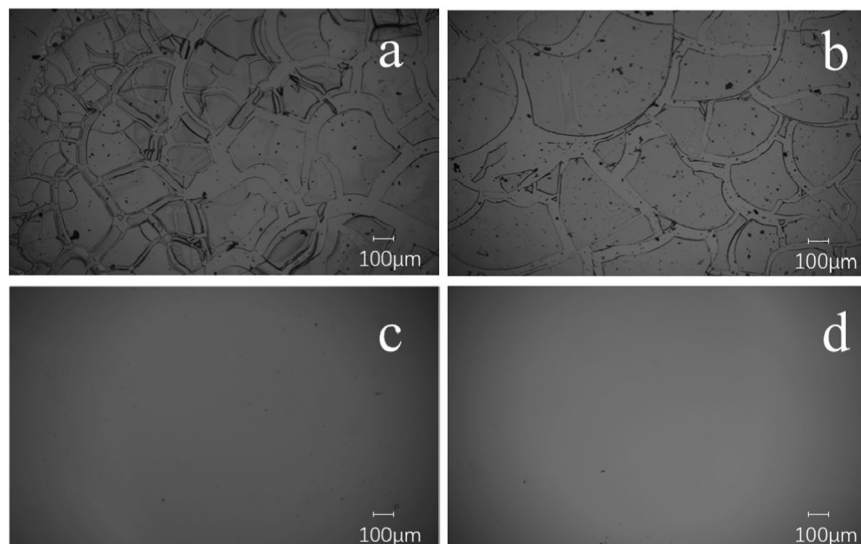


**Fig. 5** a  $^{29}\text{Si}$  NMR spectra of four kinds of organosiloxane sols; b Normalized integral intensities of the various types of Si-O bonding: branching (light gray), linearity (pattern) and termination (black) in  $^{29}\text{Si}$  NMR spectra of four organosiloxane sols

represents the number of oxygen linked to other Si atoms in each Si-O unit [40]. In our cases, only T-type and Q-type Si atoms are present, coming from three hybrid monomers and TEOS, respectively.  $^{29}\text{Si}$  NMR spectra of four sols are shown in Fig. 5a. It shows that Q-type Si atoms exist in all spectrograms as expected. A closer examination on Q-type Si atoms reveals that there is no existence of  $Q_4$  and small amount of  $Q_3$ . In hybrid sols, T-type Si atoms are mainly  $T_1$  and  $T_2$  (chemical shifts between  $-45$  and  $-63$  ppm). The lack of  $T_3$ ,  $Q_3$  and  $Q_4$  indicates that condensation is limited, as designed in this step. Further condensation is expected to occur after materials being applied on fossils.

In three hybrid sols, the molar ratio of TEOS and organosiloxanes is 1. But the number of Q-Si atoms seems much less than T-Si atoms. It may be because methoxyl groups in three organosiloxanes hydrolyze faster than the ethoxyl groups in TEOS. So part of the TEOS is not reacted and lost during evaporation. It should be aware that the sol compositions may be different from original feeding compositions. More work is still under progress in our group on this subject.

**Fig. 6** Microscopic images of films from various consolidants: **a** TEOS-s, **b** TEOS-BTME-s, **c** TEOS-TMPE-s and **d** TEOS-TMPM-s



The NMR signals of T- and Q-type Si atoms are integrated and normalized to the total integral intensity of all Si atoms in the corresponding  $^{29}\text{Si}$  NMR spectra. Based on the quantitative analysis of  $^{29}\text{Si}$  NMR data, the extent of termination ( $Q_1$ ,  $T_1$ ), linear ( $Q_2$ ,  $T_2$ ) and branching ( $Q_3$ ,  $T_3$ ) structures of polysiloxanes are further elucidated [41], as shown in Fig. 5b. The four kinds of sols are all predominantly composed of siloxane in the form of linear chains. The absence of the branched structure in TEOS-TMPM-s can be interpreted as the large steric hindrance effect caused by the acrylate groups in TMPM.

Figure 6 shows the film-forming properties of the four sols after they were coated on  $7.5 \times 2.5 \text{ cm}^2$  glass slides. Obvious cracks can be seen on films from TEOS-s and TEOS-BTME-s sols, in which cracking in film from TEOS-s is more serious. And sols of TEOS-TMPE-s and TEOS-TMPM-s can form smooth, crack-free films. As known, cracking is mainly due to the inner stress generated during sol-gel process. Apparently, organic function groups can significantly reduce the inner stress by reducing the quantity loss in the sol-gel process and proving some degree of flexibility in the final products.

### 3.3 Fossils protection evaluations

Although fossils and matrices have obvious different compositions, they show similar response to environmental changes. Thus, because of high value of fossils, evaluation experiments are normally performed on matrices as simulated fossil samples.

#### 3.3.1 Water-resistance evaluations

The fossil and matrix samples from Hami are all argillaceous rocks, which contains a large amount of water-sensitive clay

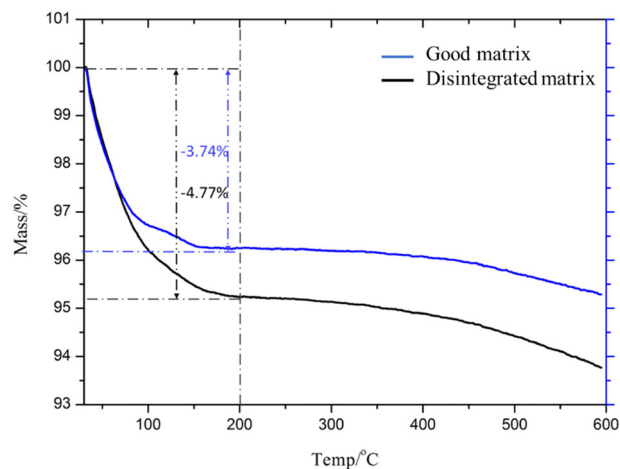


**Fig. 7** TG curves of good and disintegrated matrices

components besides quartz, calcite, apatites and feldspars. The fossils and matrices will disintegrate upon contact with water. XRD, XRF and TGA are used to compare good and disintegrated samples. XRD and XRF results indicate there are no composition and phase differences between good and disintegrated samples. As shown in Fig. 7, TGA profiles show that disintegrated sample contains 27.5% more water than original good sample. It is believed that water is the most important factor responsible for the disintegration of Hami fossils [39]. Thus, one goal of Hami fossil protection is to increase their resistance to water.

As seen in Table 4, after protective treatment the contact angles of matrices to water, all increase notably and their water absorption decrease significantly. Figure 8 visually exemplifies the water-resistance outcomes before and after protective treatments. The untreated and treated fossil samples are all placed in 10 ml of deionized water. The untreated sample falls apart immediately upon contact with water, while

the consolidants treated samples remain intact after being soaked for 12 h. It shows that the water-resistance property of the sample is greatly improved after treatment.

In Fig. 8, it can also be observed that the samples are still can be wetted nicely by water although they become more hydrophobic after treatment. This is an important issue. In the field, it allows water, from rain or other sources can still permeate into the ground after protective treatment.

### 3.3.2 Consolidation evaluations

One of the major purposes of fossil protection is consolidation. Hardness and compressive strength are used to evaluate the consolidation ability of four synthesized materials. The mechanical properties of original matrices before and after consolidation are shown in Fig. 9. After consolidation, the compressive strengths of the samples treated by polysiloxane sols all increase notably, among which hybrid sols show better consolidation results than sol of TEOS. This is because the precursors in hybrid sols have more function groups per molecule than TEOS, providing more binding/crosslinking sites (see Fig. 2).

Higher hardness can help the fossil to against wind erosion. After treatment, the Leed hardness of the samples treated by the hybrid sols increases. The sample treated by TEOS-TMPM-s has the least increase in hardness because of the larger and relatively more flexible acrylate function groups. For TEOS-s, the result is rather interesting. Since it does not

have any organic side groups, it supposes to be the most rigid. The unexpected low increase in hardness of TEOS-s is probably due to its relative weaker binding with the matrix.

### 3.3.3 Aging resistance evaluation

In Hami, strong sunlight and heat are important factors for material aging. Protected samples are placed in controlled environments to accelerate their aging processes. Color alteration is used to follow the aging. Data are summarized in Fig. 10.

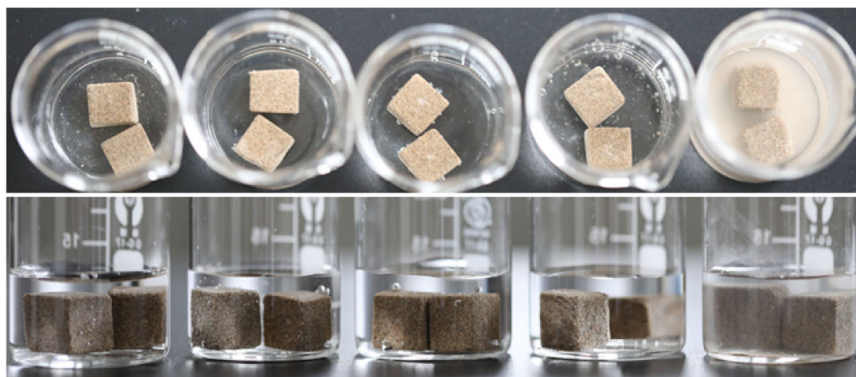
In Fig. 10a, all samples show slightly color changes in the first two days and then are almost constant later. In all samples, the  $\Delta E$  is less than 1.2, which means that all four consolidants have pretty good resistance to light. Generally,  $\Delta E < 5$  is considered to be acceptable to conservation, since such small variation will not be detected by naked eyes. The small color changes in all samples including control are probably due to water loss.

The color changes of untreated and treated samples with different consolidants, which are aged at 60 °C, are recorded in Fig. 10b. The control sample and the sample treated with TEOS-s have the least color changes, less than 1.4, since both do not have organic moieties. The color variations of the samples treated with other three consolidants are relatively larger. During heat aging,  $\Delta E$ s of TEOS-TPME-s and TEOS-TPMP-s are around 4, while  $\Delta E$  of TEOS-BTME-s is around 5. This result is not surprising, as organic components are less heat-resistant than inorganic ones. The addition of organic groups will reduce the heat resistance of materials. But overall, all four materials show decent resistance to heat aging.

**Table 4** Resistance to water of untreated and treated matrices

	Contact angle (°)	Water absorption (%)	Water resistance
Control	0	11.62 ± 0.17	Poor
TEOS-s	27.3 ± 7.5	7.11 ± 0.23	Good
TEOS-BTME-s	86.6 ± 5.3	5.15 ± 0.21	Good
TEOS-TMPE-s	104.2 ± 4.4	6.64 ± 0.19	Good
TEOS-TMPM-s	124.2 ± 3.2	6.15 ± 0.14	Good

**Fig. 8** Water-resistance test of matrices, from left to right: treated by TEOS-TMPM-s, TEOS-TMPE-s, TEOS-BTME-s, TEOS-s and control sample. Upper: top-view; Lower: side-view



## 4 Conclusions

In order to protect pterosaur fossils excavated in Hami, three hybrid polysiloxane sols and one polysiloxane sol from TEOS, a simple siloxane molecule, are synthesized via traditional sol-gel processes. TEOS is commonly used as stone

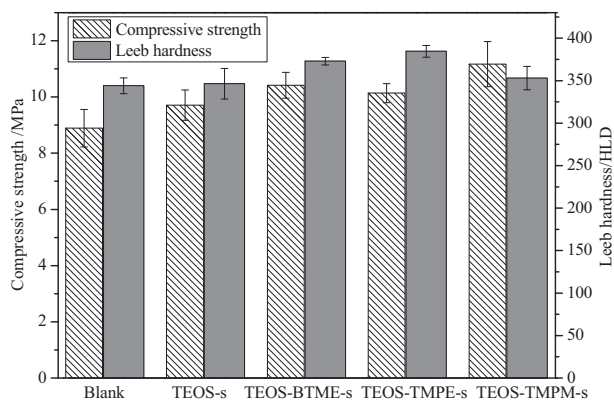


**Fig. 9** Compressive strength and Leeb hardness of the matrices before and after protective treatment

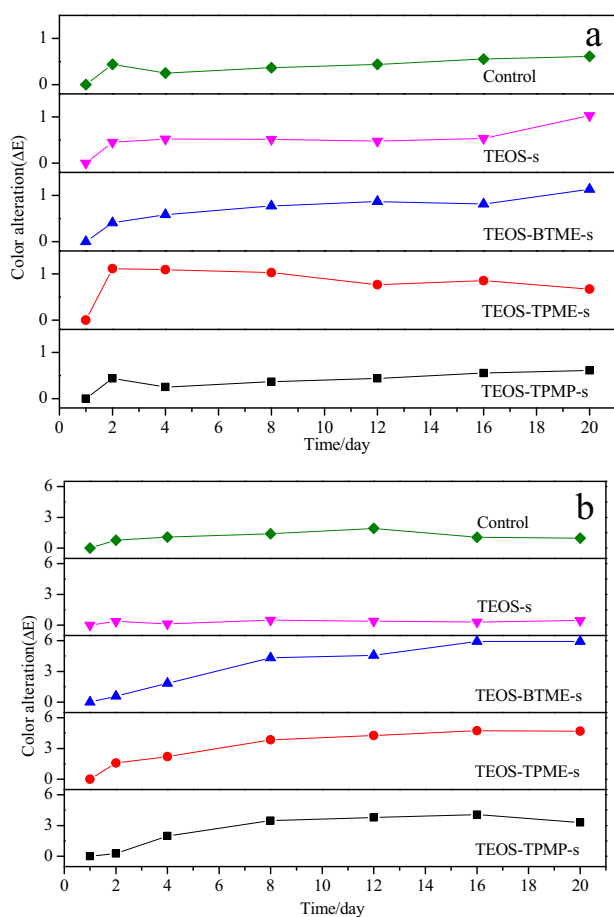


**Fig. 10** Color changes of untreated and treated matrices during aging processes. The color reference value is the color before aging. **a** Light aging was carried out at 15 cm under a UV lamp; **b** Heat aging in 60 °C oven

consolidant. It will form Si–O–Si network after sol–gel process, which can function as the binder to strengthen the stone. The results show that protection material TEOS-s from TEOS has the best aging ability against light and heat because it

lacks organic side function groups. But its abilities to increase the mechanical strength and water resistance of the fossil are relative weaker than other three hybrid materials. Meanwhile, cracking due to inner stress is always a big concern for TEOS-s.

In the hybrid sols, the organic side groups are hydrophobic and can provide extra crosslinking sites. So, the hybrid sols can strengthen the fossils and increase their resistance to water better than TEOS-s. The hybrid sols, especially TEOS-TPME-s and TEOS-TPMP-s, also show much-improved performance against cracking. This is because organic groups in hybrids further reduce the mass and volume loss during sol–gel process and provide certain degree of flexibility in the final products. The hybrid sols also show acceptable aging resistance to light and heat, although worse than TEOS-s because of the organic groups.

Our results show that siloxane-based polymers are potential protection materials for fossils. They all have their pros and cons. Attention should be paid during real case applications. But when taking all the factors into account, such as consolidation, hardness, resistance to water, light and water aging etc, hybrid sol TEOS-TPME-s shows best performance in the protection of Hami fossils.

**Acknowledgements** The authors thank Long Xiang, Yan Li, Yang Li, Shunxing Jiang, He Chen and Xinjun Zhang for their help in the field work. They are also grateful to the financial supports from the National Natural Science Foundation of China (51732008, 21673167, 41572020 and 41688103), the Innovation Project of Instrument and Equipment Function Development of the Chinese Academy of Sciences (No. 2060499), and the foundation of excavation and protection from the Hami government.

**Author contributions** All authors contributed to the study conception and design. Material preparation, data collection and analysis were performed by XP, YW and X-FM. The evaluation of fossil was performed by XP and HZ. The first draft of the manuscript was written by XP and all authors commented on previous versions of the manuscript. HB, XH, HL and XW provided the funding. All authors read and approved the final manuscript.

## Compliance with ethical standards

**Conflict of interest** The authors declare that they have no conflict of interest.

**Publisher's note** Springer Nature remains neutral with regard to jurisdictional claims in published maps and institutional affiliations.

## References

- Janvier P (2015) Facts and fancies about early fossil chordates and vertebrates. *Nature* 520(7548):483–489
- Sayani HR, Cobb KM, Cohen AL, Elliott WC, Nurhati IS, Dunbar RB, Rose KA, Zaunbrecher LK (2011) Effects of diagenesis on paleoclimate reconstructions from modern and young fossil corals. *Geochim Cosmochim Acta* 75(21):6361–6373



3. Zhang C, Guo Z, Deng C, Ji X, Wu H, Paterson GA, Chang L, Li Q, Wu B, Zhu R (2016) Clay mineralogy indicates a mildly warm and humid living environment for the Miocene hominoid from the Zhaotong Basin, Yunnan, China. *Sci Rep* 6:20012
4. Buncea M, Worthy TH, Phillips MJ, Holdaway RN, Willerslev E, Haile J, Shapiro B, Drummond A, Scofield RP, Kamp PJJ, Cooper A (2009) The evolutionary history of the extinct ratite moa and New Zealand Neogene paleogeography. *Proc Natl Acad Sci USA* 106(49):20646–20651
5. Menningen J, Siegesmund S, Tweeton D, Träupmann M (2018) Ultrasonic tomography: non-destructive evaluation of the weathering state on a marble obelisk, considering the effects of structural properties. *Environ Earth Sci* 77(17):601
6. Salman AB, Howari FM, El-Sankary MM, Wali AM, Saleh MM (2010) Environmental impact and natural hazards on Kharga Oasis monumental sites, Western Desert of Egypt. *J Afr Earth Sci* 58(2):341–353
7. Bonazza A, Messina P, Sabbioni C, Grossi CM, Brimblecombe P (2009) Mapping the impact of climate change on surface recession of carbonate buildings in Europe. *Sci Total Environ* 407(6):2039–2050
8. Cardell C, Delalieux F, Roumpopoulos K, Moropoulou A, Auger F, Van Grieken R (2003) Salt-induced decay in calcareous stone monuments and buildings in a marine environment in SW France. *Constr Build Mater* 17(3):165–179
9. E. Ruiz-Agudo FM, Jacobs P, Rodriguez-Navarro C (2007) The role of saline solution properties on porous limestone salt weathering by magnesium and sodium sulfates. *Environ Geol* 52(2):269–281
10. McNamara CJ, Perry TDt, Bearce KA, Hernandez-Duque G, Mitchell R (2006) Epilithic and endolithic bacterial communities in limestone from a Maya archaeological site. *Micro Ecol* 51(1):51–64
11. Bracci S (2001) Lidar remote sensing of stone cultural heritage: detection of protective treatments. *Optical Eng* 40(8):1579–1583
12. Xu F, Tang J, Gao S (2010) Characterization and origin of weathering crusts on Kylin carved-stone, Kylin countryside, Nanjing – a case study. *J Cultural Herit* 11(2):228–232
13. Xu F, Zeng W, Li D (2019) Recent advance in alkoxy silane-based consolidants for stone. *Prog Org Coat* 127:45–54
14. Temraz MG, Khallaf MK (2016) Weathering behavior investigations and treatment of Kom Ombo temple sandstone, Egypt – based on their sedimentological and petrographical information. *J Afr Earth Sci* 113:194–204
15. Ludovico-Marques M, Chastre C (2014) Effect of consolidation treatments on mechanical behaviour of sandstone. *Constr Build Mater* 70:473–482
16. Baud P, Zhu W, Wong T-F (2000) Failure mode and weakening effect of water on sandstone. *J Geophys Res Solid Earth* 105(B7):16371–16389
17. Zhang H, Liu Q, Liu T, Zhang B (2013) The preservation damage of hydrophobic polymer coating materials in conservation of stone relics. *Prog Org Coat* 76(7–8):1127–1134
18. Eyssautier-Chuine S, Marin B, Thomachot-Schneider C, Fronteau G, Schneider A, Gibeaux S, Vazquez P (2016) Simulation of acid rain weathering effect on natural and artificial carbonate stones. *Environ Earth Sci* 75(9)
19. Delalieux F, Todorov V, Dekov VM, Grieken RV (2001) Environmental conditions controlling the chemical weathering of the Madara Horseman monument, NE Bulgaria. *J Cultural Herit* 2(1):43–54
20. Maravelaki-Kalaitzaki P, Kallithrakas-Kontos N, Agioutantis Z, Maurigiannakis S, Korakaki D (2008) A comparative study of porous limestones treated with silicon-based strengthening agents. *Prog Org Coat* 62(1):49–60
21. Rodrigues JD, Grossi A (2007) Indicators and ratings for the compatibility assessment of conservation actions. *J Cultural Herit* 8(1):32–43
22. Franzoni E, Graziani G, Sassoni E (2015) TEOS-based treatments for stone consolidation: acceleration of hydrolysis–condensation reactions by poulticing. *J Sol-Gel Sci Technol* 74(2):398–405
23. Grissom CA, Charola AE, Boulton A, Mecklenburg MF (2013) Evaluation over time of an ethyl silicate consolidant applied to ancient lime plaster. *Stud Conserv* 44(2):113–120
24. Saleh AS, Helmi FM, Monir MK, El-Banna A-FE (1992) Study and consolidation of sandstone: temple of Karnak, Luxor, Egypt. *Stud Conserv* 37(2):93–104
25. Mosquera MJ, Pozo J, Esquivias L, Rivas T, Silva B (2002) Application of mercury porosimetry to the study of xerogels used as stone consolidants. *J Non Cryst Solids* 311(2):185–194
26. Mosquera MJ, Pozo J, Esquivias L (2003) Stress during drying of two stone consolidants applied in monumental conservation. *J Sol-Gel Sci Technol* 26(1–3):1227–1231
27. Lehmann RG, Miller JR, Kozerski GE (2000) Degradation of silicone polymer in a field soil under natural conditions. *Chemosphere* 41(5):743–749
28. Liu R, Han X, Huang X, Li W, Luo H (2013) Preparation of three-component TEOS-based composites for stone conservation by sol–gel process. *J Sol-Gel Sci Technol* 68(1):19–30
29. Mosquera MJ, de los Santos DM, Montes A, Valdez-Castro L (2008) New nanomaterials for consolidating stone. *Langmuir* 24(6):2772–2778
30. Mosquera MJ, de los Santos DM, Valdez-Castro L, Esquivias L (2008) New route for producing crack-free xerogels: obtaining uniform pore size. *J Non Crystal Solids* 354(2–9):645–650
31. Alié C, Pirard R, Lecloux AJ, Pirard J-P (1999) Preparation of low-density xerogels through additives to TEOS-based alcogels. *J Non Crystal Solids* 246(3):216–228
32. Xu F, Li D, Zhang H, Peng W (2011) TEOS/HDMS inorganic–organic hybrid compound used for stone protection. *J Sol-Gel Sci Technol* 61(2):429–435
33. Zárraga R, Cervantes J, Salazar-Hernandez C, Wheeler G (2010) Effect of the addition of hydroxyl-terminated polydimethylsiloxane to TEOS-based stone consolidants. *J Cultural Herit* 11(2):138–144
34. Zárraga R, Alvarez-Gasca DE, Cervantes J (2002) Solvent effect on TEOS film formation in the sandstone consolidation process. *Silicon Chem* 1(5–6):397–402
35. Wang X, Kellner AWA, Jiang S, Wang Q, Ma Y et al. (2014) Sexually dimorphic tridimensionally preserved pterosaurs and their eggs from China. *Curr Biol* 24:1323–1330
36. Wang X, Kellner AWA, Jiang S, Cheng X, Wang Q et al. (2017) Egg accumulation with 3D embryos provides insight into the life history of a pterosaur. *Science* 358:1197–1201
37. David M, Martill (2014) Palaeontology: which came first, the pterosaur or the egg? *Curr Biol* 24:R615–R617
38. Deeming DC (2017) Palaeontology: how pterosaurs bred. *Science* 358:1124–1125
39. Wenhua Z, Xiangna H, Cong C, Xiaolin W (2019) Studies on salt weathering of hami fossils in Xinjiang, The 9th Graduate Student’s Forum on Archaeology in Beijing
40. Wang S-D, Scrivener KL (2003) <sup>29</sup>Si and <sup>27</sup>Al NMR study of alkali-activated slag. *Cem Concr Res* 33(5):769–774
41. Hall CJ, Ponnusamy T, Murphy PJ, Lindberg M, Antzutkin ON, Griesser HJ (2014) A solid-state nuclear magnetic resonance study of post-plasma reactions in organosilicone microwave plasma-enhanced chemical vapor deposition (PECVD) coatings. *ACS Appl Mater Interfaces* 6(11):8353–8362